Supplementary Information (SI) for Journal of Materials Chemistry A.

Chromium and Nitrogen co-facilitating NiMo-based catalyst achieving high-efficiency and durable intermittent water electrolysis

Qilong Liu,[a] Qizhu Qian,[b] Huiyi Li,[b] Mengxiang Wang,[b] Jujia Zhang,[a] Mingliang Fang,[a] Wei Bai,[a] and Wentuan Bi [a*]

[a] Institute of Energy, Hefei Comprehensive National Science Center (Anhui Energy Laboratory), Hefei, Anhui, 230031, P. R. China

[b] Hefei National Research Center for Physical Sciences at the Microscale, University of Science and Technology of China, Hefei, Anhui, 230026, P. R. China

[*] Represents the corresponding author

Materials

Nitric acid nickel(II) hexahydrate ($Ni(NO_3)_2 \cdot 6H_2O$, AR, ⩾98.0%), ammonium molybdate tetrahydrate ($(NH_4)_6Mo_7O_{24} \cdot 4H_2O$, AR, ⩾99.0%), chromium(III) chloride hexahydrate ($CrCl_3 \cdot 6H_2O$, AR, ⩾99.0%), potassium hydroxide (KOH), urea ($CO(NH_2)_2$), and hydrochloric acid (HCl, AR, 36.0%–38.0%) were purchased from Sinopharm Chemical Reagent Co.,Ltd. All chemical reagents were used without any further purification. The distilled water used in all experiments was purified by a Millipore system (18.25 MΩ·cm).

Figure S 1 Diagram of nitriding treatment.

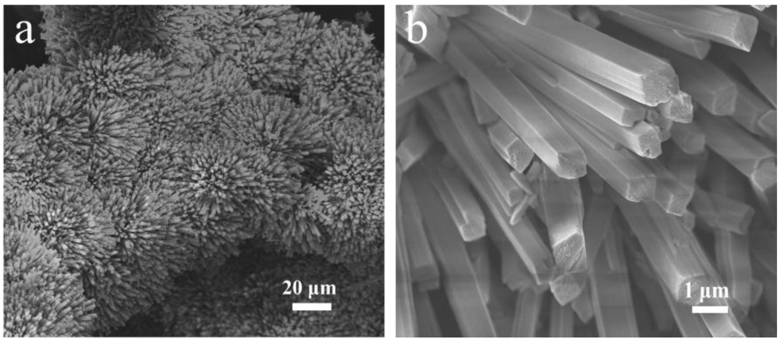

Figure S 2 （a）and (b) SEM images of NiMo/NF.

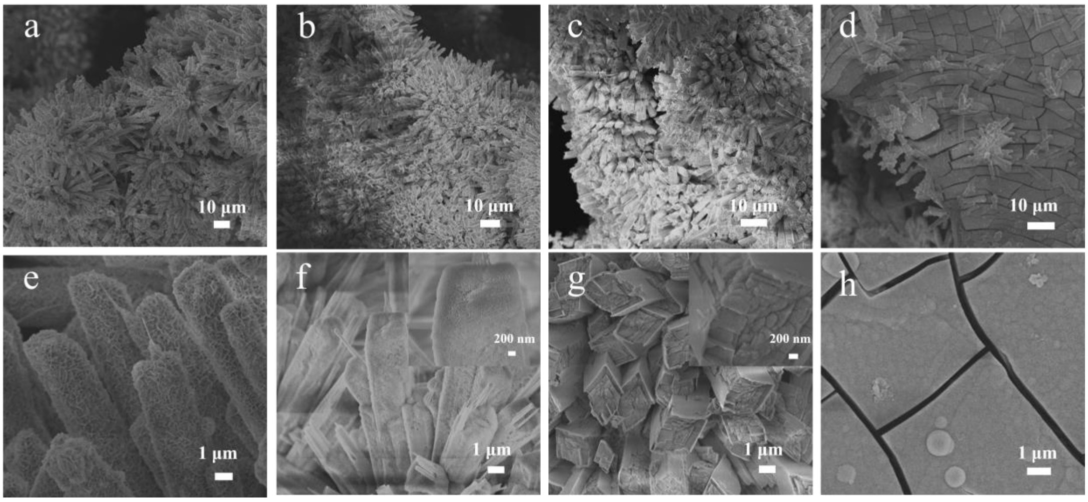

Figure S 3 SEM images of (a) and (e) NiMoCr(1)/NF; (b) and (f) NiMoCr(3)/NF; (c) and (g) NiMoCr(5)/NF; (d) and (h) NiMoCr(7)/NF.

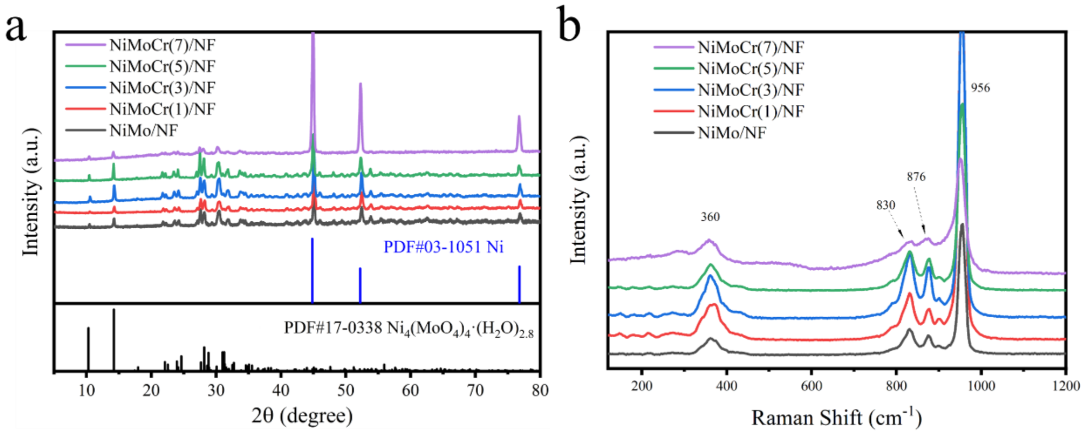

Figure S 4 (a) XRD pattern and (b) Raman spectrum of NiMo/NF, NiMoCr(1)/NF, NiMoCr(3)/NF NiMoCr(5)/NF and NiMoCr(7)/NF.

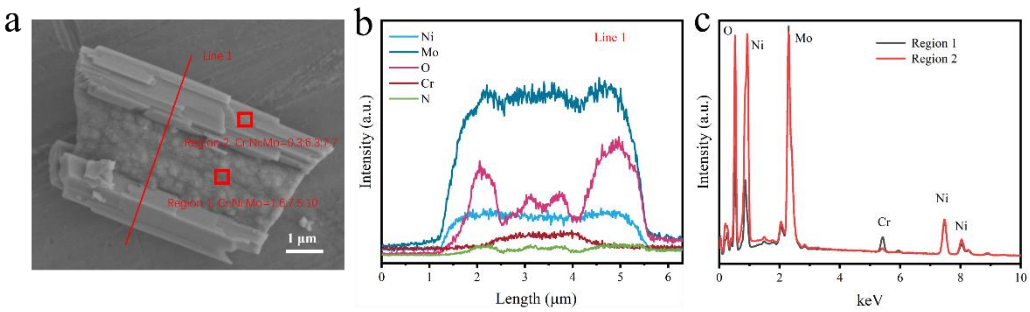

Figure S 5 (a) SEM image of NiMoCr(5)-N/NF, along with the designated positions for line and point scans; EDS data are provided in (b) for line scanning and in (c) for point scanning.

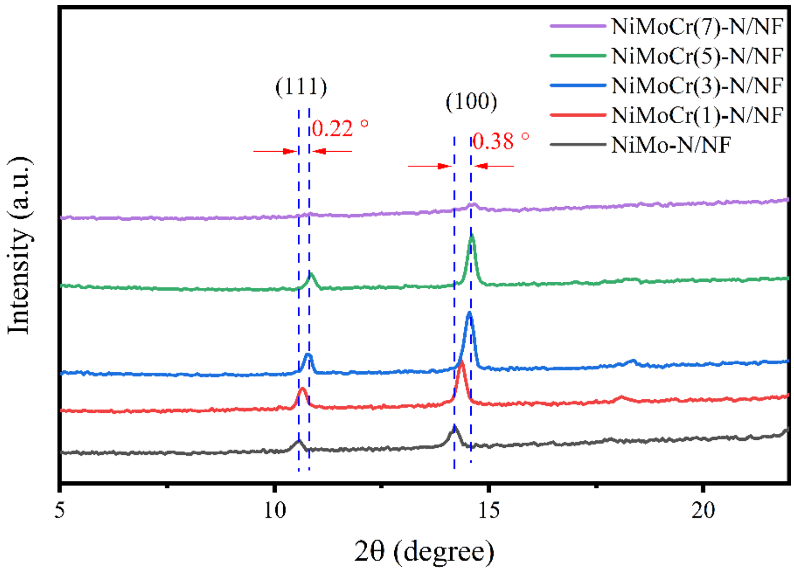

Figure S 6 The expanded XRD pattern from 5 to 22°.

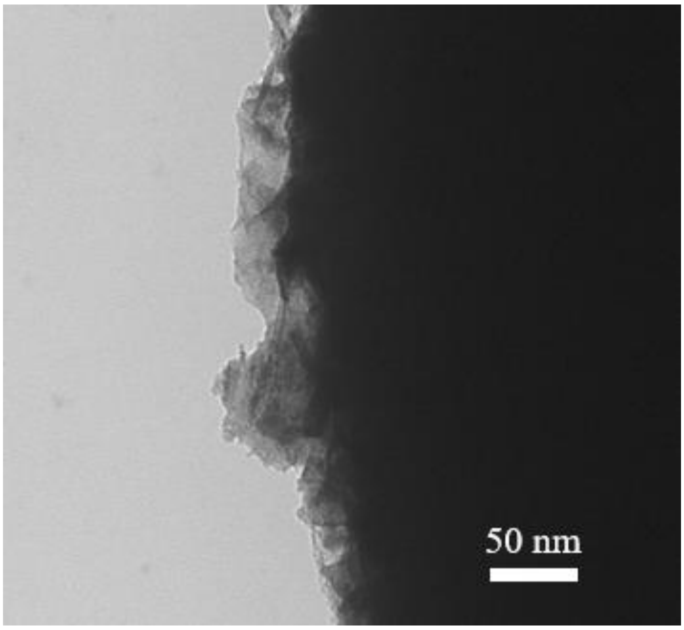

Figure S 7 TEM image of NiMoCr(3)-N/NF.

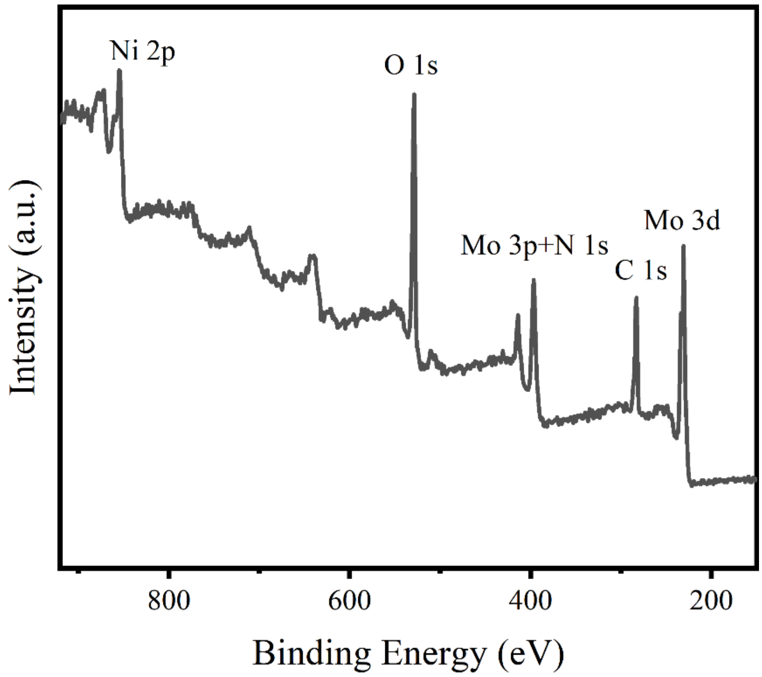

Figure S 8 The survery XPS spectra of NiMoCr(3)-N/NF.

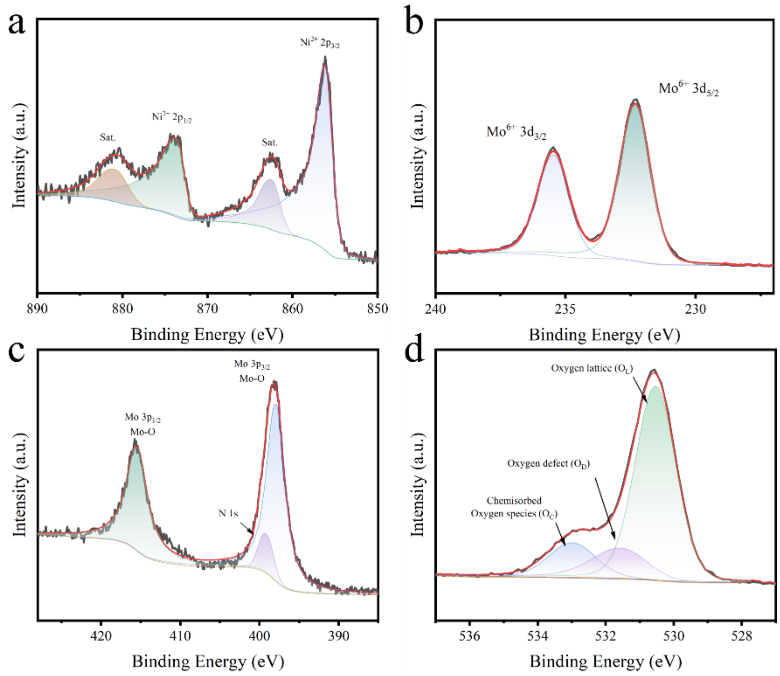

Figure S 9 High resolution XPS spectrum of NiMo/NF. (a) Ni 2p; (b) Mo 3d; (c) N 1s and Mo 3p; and (d) O 1s..

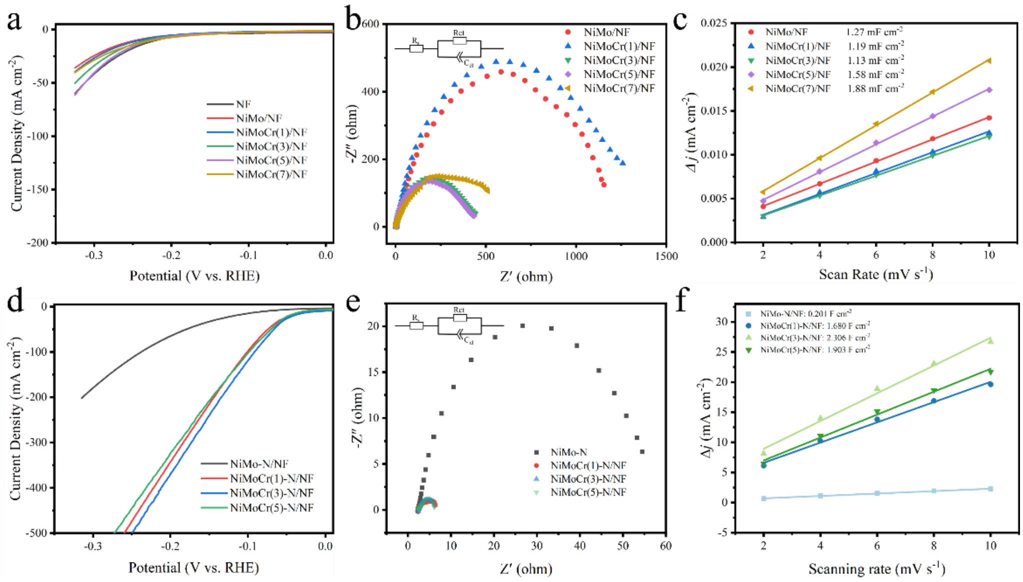

Figure S 10 (a) LSV curves; (b) EIS; (c) Cdl curves for NF, NiMo/NF, NiMoCr(1)/NF, NiMoCr(3)/NF, NiMoCr(5)/NF and NiMoCr(7)/NF. (d) LSV curves; (e) EIS; (f) Cdl curves for NiMo-N/NF, NiMoCr(1)-N/NF, NiMoCr(3)-N/NF, and NiMoCr(5)-N/NF.

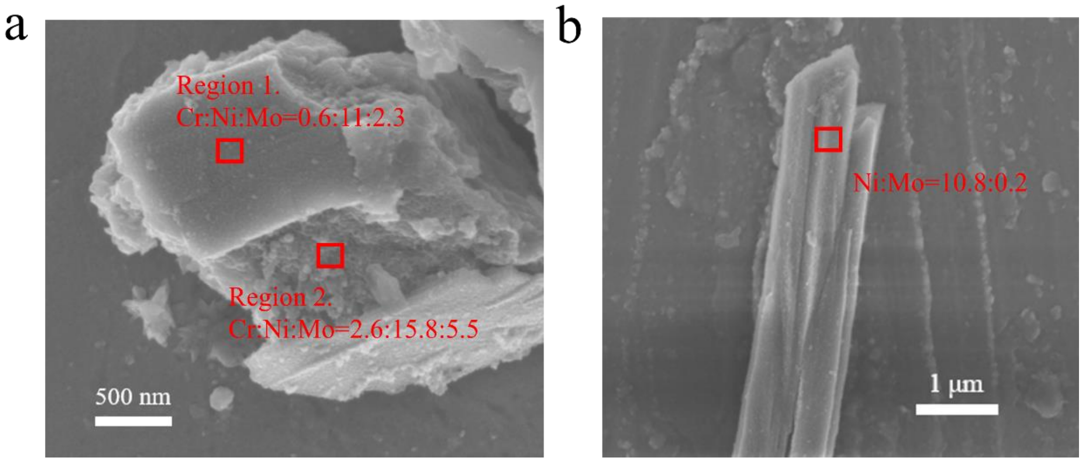

Figure S 11 SEM images of post-reaction (a) NiMoCr(5)-N/NF and (b) NiMo-N/NF electrodes and the corresponding DES spots scanning region.

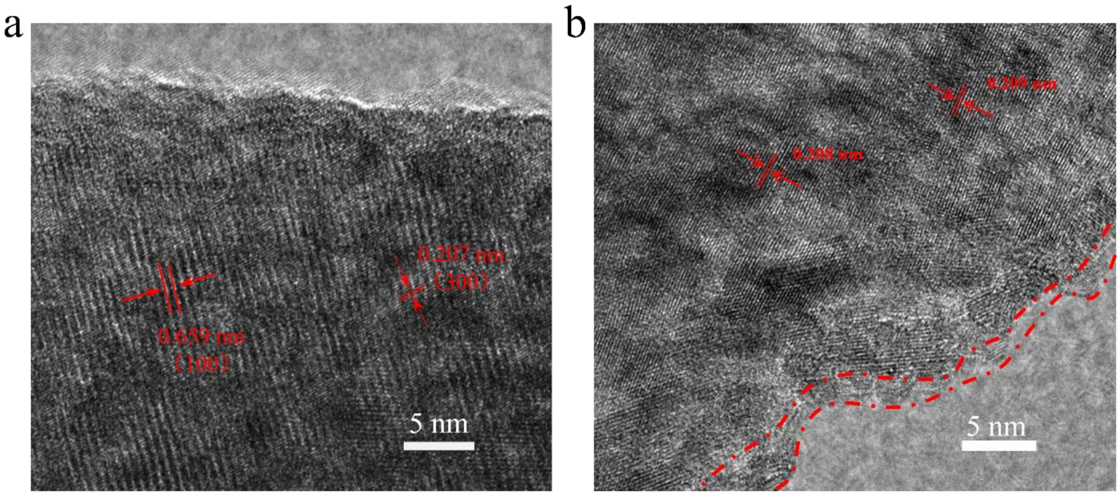

Figure S 12 the compared HRTEM images of (a) pre-reaction NiMoCr(3)-N/NF and (b) post-reaction NiMoCr(3)-N/NF.

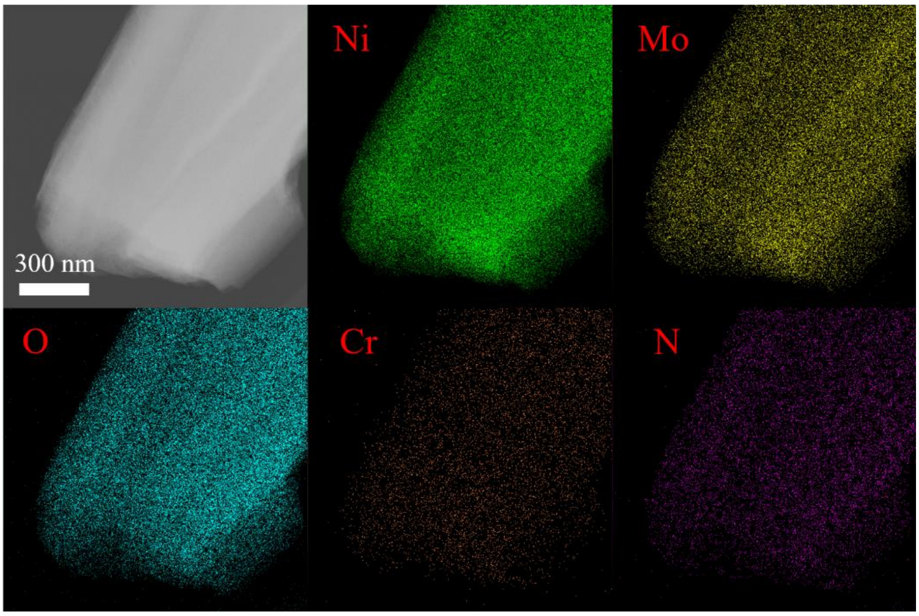

Figure S 13 The EDS mapping of the post-reaction NiMoCr(3)-N/NF.

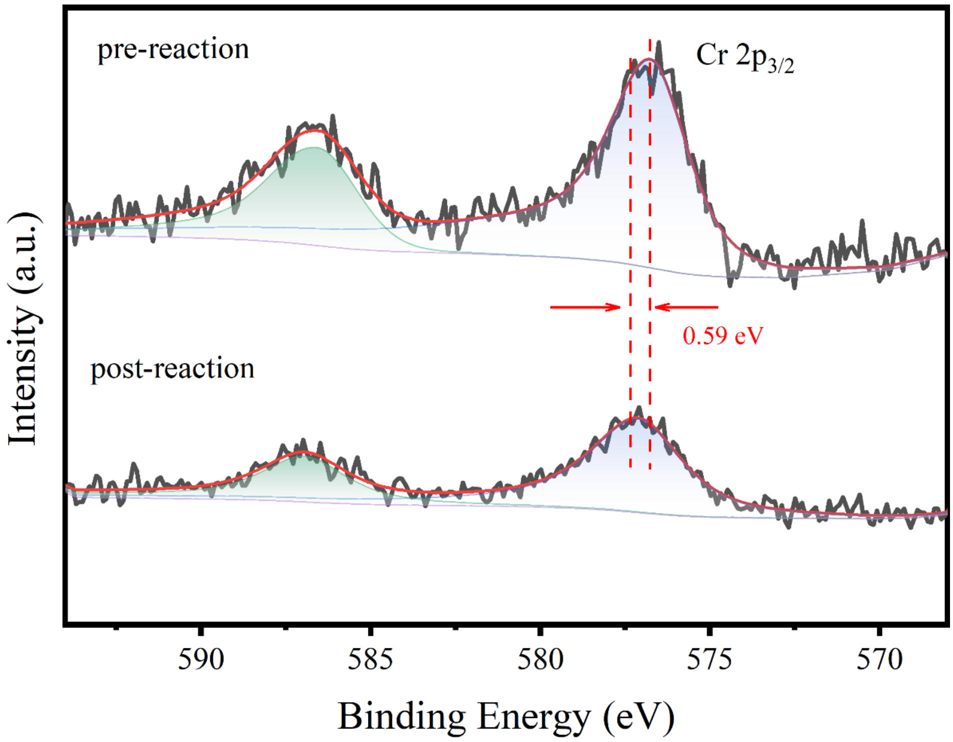

Figure S 14 High resolution XPS for Cr 2p of pre- and post-reaction of NiMoCr(5)-N/NF.

Table S 1 The HER performance of transition metal-based catalysts in 1 M KOH.

Catalysts	Overpotential (mV@ mA cm^{-2})	Tafel slop (mV dec^{-1})	Ref.
NiMoCr-N/NF	92 mV @ 100 mA cm^{-2}	64	This work
Ni_2Mo_3N/NF	21.3 mV @ 10 mA cm^{-2} 123.8 mV @100 mA cm^{-2}	62	1
S-$NiFe_2O_4$/NF	138 mV @ 10 mA cm^{-2}	61	2
Ni_3S_2 NA/NF	200 mV @10 mA cm^{-2}	107	3
Ni_3S_2@MoS_2/FeOOH	95 mV @ 10 mA cm^{-2}	85	4
Ni-Fe-MoN NTs	55 mV @ 10 mA cm^{-2} 199 mV @ 100 mA cm^{-2}	109	5
V-$Ni_{0.2}Mo_{0.8}N$	39 mV @ 10 mA cm^{-2} 178 mV @ 200 mA cm^{-2}	37.7	6
Ni@NCNT/NiMoN/NF	15 mV @10 mA cm^{-2} 156 mV @ 100 mA cm^{-2}	68	7
N-$NiMoO_4$/NiS_2	57 mV @ 10 mA cm^{-2}	74.2	8
Ni_3N-NiMoN	31 mV @10 mA cm^{-2} 210 mV @ 100 mA cm^{-2}	64	9
NiMo HNRs/TiM	92 mV @10 mA cm^{-2} 200 mV @ 100 mA cm^{-2}	47	10
$Ni(PO_3)_2$–MoO_3/NF	86 mV @10 mA cm^{-2} 205 mV @ 100 mA cm^{-2}	50.1	11
NiMo NWs/Ni	30 mV @10 mA cm^{-2} 125 mV @ 100 mA cm^{-2}	86	12
$NiCo_2P_x$	58 mV @10 mA cm^{-2} 127 mV @ 100 mA cm^{-2}	34.3	13
C-Ni_3S_2/NF	89 mV @10 mA cm^{-2} 186 mV @ 100 mA cm^{-2}	85	14
NF@Ni/C-600	37 mV @10 mA cm^{-2} 124 mV @ 50 mA cm^{-2}	57	15

1. S. H. Park, T. H. Jo, M. H. Lee, K. Kawashima, C. B. Mullins, H.-K. Lim and D. H. Youn, *Journal of Materials Chemistry A*, 2021, **9**, 4945-4951.
2. J. Liu, D. Zhu, T. Ling, A. Vasileff and S.-Z. Qiao, *Nano Energy*, 2017, **40**, 264-273.
3. C. Ouyang, X. Wang, C. Wang, X. Zhang, J. Wu, Z. Ma, S. Dou and S. Wang, *Electrochimica Acta*, 2015, **174**, 297-301.
4. M. Zheng, K. Guo, W.-J. Jiang, T. Tang, X. Wang, P. Zhou, J. Du, Y. Zhao, C. Xu and J.-S. Hu, *Applied Catalysis B: Environmental*, 2019, **244**, 1004-1012.
5. C. Zhu, Z. Yin, W. Lai, Y. Sun, L. Liu, X. Zhang, Y. Chen and S.-L. Chou, *Advanced Energy Materials*, 2018, **8**, 1802327.
6. P. Zhou, X. Lv, D. Xing, F. Ma, Y. Liu, Z. Wang, P. Wang, Z. Zheng, Y. Dai and B. Huang, *Applied Catalysis B: Environmental*, 2020, **263**, 118330.
7. Y. Gong, L. Wang, H. Xiong, M. Shao, L. Xu, A. Xie, S. Zhuang, Y. Tang, X. Yang, Y. Chen and P. Wan, *Journal of Materials Chemistry A*, 2019, **7**, 13671-13678.
8. L. An, J. Feng, Y. Zhang, R. Wang, H. Liu, G.-C. Wang, F. Cheng and P. Xi, *Advanced Functional Materials*, 2019, **29**, 1805298.
9. A. Wu, Y. Xie, H. Ma, C. Tian, Y. Gu, H. Yan, X. Zhang, G. Yang and H. Fu, *Nano Energy*, 2018, **44**, 353-363.
10. J. Tian, N. Cheng, Q. Liu, X. Sun, Y. He and A. M. Asiri, *Journal of Materials Chemistry A*, 2015, **3**, 20056-20059.
11. K. Li, J. Ma, X. Guan, H. He, M. Wang, G. Zhang, F. Zhang, X. Fan, W. Peng and Y. Li, *Nanoscale*, 2018, **10**, 22173-22179.
12. M. Fang, W. Gao, G. Dong, Z. Xia, S. Yip, Y. Qin, Y. Qu and J. C. Ho, *Nano Energy*, 2016, **27**, 247-254.
13. R. Zhang, X. Wang, S. Yu, T. Wen, X. Zhu, F. Yang, X. Sun, X. Wang and W. Hu, *Advanced Materials*, 2017, **29**, 1605502.
14. J. Zhang, Y. Li, T. Zhu, Y. Wang, J. Cui, J. Wu, H. Xu, X. Shu, Y. Qin, H. Zheng, P. M. Ajayan, Y. Zhang and Y. Wu, *ACS Applied Materials & Interfaces*, 2018, **10**, 31330-31339.
15. H. Sun, Y. Lian, C. Yang, L. Xiong, P. Qi, Q. Mu, X. Zhao, J. Guo, Z. Deng and Y. Peng, *Energy & Environmental Science*, 2018, **11**, 2363-2371.